Polypropylene filled with activated carbon from palm kernel shells as antistatic packaging

Mujtahid Kaavessina[1), *)] (ORCID ID: 0000-0003-0630-4497), **Sperisa Distantina**[1)] (0000-0002-8726-7191), **Muhamad Rizki Hi. Wahab**[1)], **Natasya Yola Ferdilla**[1)], **Joko Waluyo**[1)] (0000-0001-6721-0473)

DOI: https://doi.org/10.14314/polimery.2025.4.4

Abstract: Effect of activated carbon (AC) obtained from palm kernel shells on the electrical conductivity of polypropylene (PP) intended for antistatic packaging was investigated. AC (1–4 wt%) was introduced into PP by solution mixing. FT-IR analysis confirmed the absence of new functional groups, and SEM showed uniform distribution of the filler in the polymer matrix. Electrical conductivity was increasing with increased AC content (8.01×10^{-10} S/m for 4 wt% of AC), approaching the limit required for antistatic materials. In addition, tensile strength was increasing with simultaneous reduction of elongation and increase of crystallinity degree and thermal stability. At a higher AC content (4 wt%), agglomerate formation was observed, which slightly deteriorated mechanical and electrical properties. The results indicate that with an appropriately selected filler content, PP composites with AC additives can be a promising material for antistatic packaging.

Keywords: PP, activated carbon, palm kernel shells, solvent method, antistatic packaging.

Polipropylen napełniony węglem aktywnym z łupin palmowych jako antystatyczne opakowania

Streszczenie: Zbadano wpływ węgla aktywnego (AC) otrzymanego z odpadów łupin palmowych na przewodność elektryczną polipropylenu (PP) przeznaczonego na opakowania antystatyczne. AC (0–4% mas.; <74 μm) wprowadzano do PP metodą mieszania w roztworze. Analiza FT-IR potwierdziła brak nowych grup funkcyjnych, a SEM wykazała równomierne rozmieszczenie napełniacza w osnowie polimerowej. Przewodność elektryczna zwiększała się wraz z zawartością AC ($8,01 \times 10^{-10}$ S/m dla 4% mas z AC), zbliżając się do granicy wymaganej dla materiałów antystatycznych. Ponadto zwiększała się wytrzymałość na rozciąganie przy jednoczesnym zmniejszeniu wydłużenia oraz zwiększeniu stopnia krystaliczności i stabilności cieplnej. Przy większej zawartości AC (4% mas.) zaobserwowano tworzenie się aglomeratów, co nieznacznie pogorszyło właściwości mechaniczne i elektryczne. Wyniki wskazują, że przy odpowiednio dobranym udziale napełniacza kompozyty PP z dodatkiem AC mogą być obiecującym materiałem na opakowania antystatyczne.

Słowa kluczowe: PP, węgiel aktywny, łupiny orzecha palmowego, metoda rozpuszczalnikowa, opakowania antystatyczne.

Electronics are vulnerable to harm from electrostatic discharge, hence necessitating the usage of antistatic packaging during distribution. Antistatic packaging is designed to protect electronic products against physical, environmental, and electrostatic discharge (ESD) harm. Electrostatic discharge (ESD) can happen when electric charge is transferred between objects with varying electrostatic potentials. ESD can lead to performance degradation, unpredictable operation, and potential malfunction [1].

Polymer materials are commonly used for packaging due to their stability, lightweight, and affordability [2, 3]. Polypropylene (PP) is a widely used polymer for packaging and exhibits robustness, hardness, chemical resistance, malleability under heat treatment, non-corrosiveness, recyclability, and affordability [4]. These properties suggest that PP has the potential to be utilized as a material for producing antistatic packaging. Nevertheless, the electrical conductivity of PP is exceedingly low, necessitating adjustments to be made to alter it. One method of modifying the characteristics of polymers is by incorporating fillers. However, evaluating any potential impact on other properties that could be compromised is imperative [5].

Carbon-based filler materials such as carbon black, graphite, graphene, and carbon nanotubes have been proven to enhance the electrical conductivity of polymer matrices such as polylactic acid, epoxy resin, polyethyl-

---

[1)] Chemical Engineering, Faculty of Engineering, Universitas Sebelas Maret, Surakarta 57125, Indonesia.

[*)] Author for correspondence: mkaavessina@staff.uns.ac.id

ene, etc. [6–8]. This improvement arises from developing conductive networks within the polymer matrix, facilitating effective electron transport. The improved characteristics of carbon-filled polymers make them appropriate for various applications, such as electronic devices, antistatic packaging, energy storage systems, and thermal management solutions in microelectronics [9–11]. Some researchers also concluded that the dispersion and alignment of fillers inside the polymer matrix are crucial for improving the properties of the composites, such as thermal and electrical conductivity [8, 11].

The above explanations encourage the investigation of carbon-based fillers such as activated carbon (AC). Palm kernel shell (PKS) waste is one of the most promising sources of AC, which can be obtained from natural materials that contain hemicellulose. Data from the Central Bureau of Statistics (2021) indicates that Indonesia produces 46.2 million tons of oil palm fresh fruit bunches. One ton of oil palm fresh fruit bunches generates trash of 23% empty oil palm bunches, 6.5% shell waste, 4% wet decanter solids, 13% fiber, and 50% liquid waste [12–14].

PKS has been commonly utilized as conventional fuel. Consequently, it is imperative to increase its economic value by transforming it into AC as a filler in the polymer matrix. This research utilizes AC from PKS as a filler of PP to produce more economical antistatic packaging. AC (less than 74 μm) was incorporated into PP using a solvent method with m-xylene as a solvent, hereinafter designated as PP micro-composites. The main objective of this work is to determine the electrical conductivity of PP micro-composites that meet the criteria of antistatic material. Other properties of PP micro-composites were investigated to determine whether there were changes in mechanical and thermal properties of PP with the presence of filler.

EXPERIMENTAL PARTS

Materials

Polypropylene (PP) with a melt flow rate (MFR) of 12 g/10 min (ASTM D1238) and a melting point of 165°C was supplied by PT Polytama Propindo (Jawa Barat, Indonesia) under the trade name Masplene 5402. Palm kernel shells (PKS) were purchased from the local market in Indonesia. M-xylene (96%) and NaOH were purchased from Sigma Aldrich (Germany). All compounds were used without any purification.

Methods

Preparation of activated carbon from palm kernel shell waste

PKS was washed, cleaned and after drying, crushed with a disc mill, and then carbonated in an oven at 500°C for 2 h. The carbon was crushed and sieved until it reached a size that passed through a 200-mesh sieve (< 74 μm). The activation step was subsequently conducted by adding 1 M NaOH, followed by stirring and sealing for 24 h. The products were filtered, rinsed with distilled water, and dried in an oven at 100°C for 3 h.

Preparation of PP micro-composites by solvent method

The preparation of PP micro-composites using solvent method consisted of dissolving 30 g of PP in 100 mL of m-xylene (180°C) and then stirring for 3 h. Then, AC obtained from PKS was added and stirred for 1 h in different proportions (Table 1). The mixture was poured into a glass mold and left at room temperature for the solvent to evaporate (24 h). To produce the ASTM standard test samples, the dried PP micro-composite sheets were cut into small pieces and fed into the injection molding machine.

Characterization

To evaluate the functional groups that may be formed during the mixing process, ATR-FT-IR spectroscopy analysis (Bruker Vertex 70 instrument, Germany) was performed using 32 scans, a resolution of 4 cm^{-1} and a wavenumber range of 4000–400 cm^{-1}. Morphology was determined by scanning electron microscopy (SEM), JEOL JSM-6360A, Japan, at 15kV. The electrical conductivity was determined using a ZC-90G insulation resistance meter using the two-probe method. The configuration of this equipment is depicted schematically in Figure 1. The electrical resistivity (r) of the samples was determined by measuring the direct-current (DC) resistance (R) along the entire length of the samples. Subsequently, the conductivity is assessed by determining the resistivity of the sample using Equations 1 and 2.

$$\varrho = \frac{R \cdot A}{l} \tag{1}$$

$$\sigma = \frac{1}{\varrho} \tag{2}$$

T a b l e 1. PP micro-composites preparation

Sample	Polypropylene, g	m-xylene, mL	Activated carbon, g
Pure PP	30.0	120	0
PP/PKS1	29.7	120	0.3
PP/PKS2	29.4	120	0.6
PP/PKS3	29.1	120	0.9
PP/PKS4	28.8	120	1.2

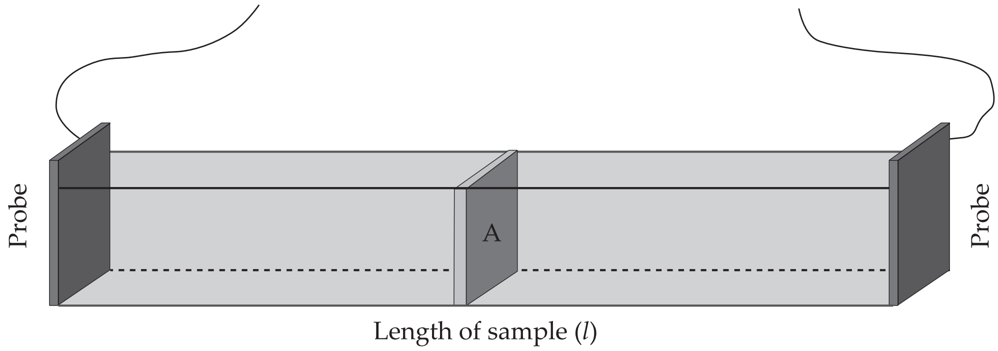

Fig. 1. Schematic setup for measuring the DC resistance of the sample

where: σ is electrical conductivity (S/m), ϱ is resistivity (Ω · m), A is cross-sectional area (1.09 × 10^{-5} m^2), and *l* is the length of the sample (0.02 m).

Mechanical properties were conducted using Dongguan Lixian Instrument Scientific's HZ-1007A (Dongguan, China) in accordance with ASTM D-638 (test samples type IV). The gauge length and the strain rate were prescribed at 50 mm and 50 mm/min, respectively. The average data is obtained by analyzing three specimens of each sample at ambient temperature. Thermal properties of PP micro-composites were assessed using a simultaneous TGA-DSC measurements, Nexta STA (Hitachi STA200RV, Tokyo, Japan) at a heating rate of 10°C/min, within the temperature range 30–500°C, and under a nitrogen atmosphere. The degree of crystallinity (X_c) is calculated using Equation 3:

$$X_c = \frac{\Delta H_m}{\Phi \cdot \Delta H_m^0} \cdot 100 \qquad (3)$$

where: ΔH_m is the melting enthalpy of the sample (J/g), *F* is the weight fraction of PP, and ΔH_m^{o} is the melting enthalpy value of pure PP, which is 207 J/g [22].

RESULTS AND DISCUSSION

ATR-FT-IR analysis was conducted to evaluate the existence of m-xylene residue and the possibility of new functional groups formed during the blending process. Figure 2 presents the ATR-FT-IR spectra of pure PP and PP micro-composites. All patterns exhibited similar forms, except for the peak at 1620 cm^{-1}, which was exclusively observed in PP micro-composites. The occurrence of peaks that solely appear in micro-composites signifies the presence of AC [15]. Overall, it can be observed that there are no significant differences between the spectra of pure PP and PP micro-composites in the organic compound range (400–4000 cm^{-1}). It can be assumed that m-xylene has completely evaporated from the sample.

Polypropylene is synthesized from the monomer propylene, wherein the carbon double bond (C=C) undergoes a reaction to form polymer chains. The repeating unit of PP comprises a $-CH_2$ and a $-CH_3$ groups. The methyl group is referred to as a pendant group because it is not incorporated into the polymer chain but branches from it. Figure 3 illustrates that PP exhibits $-CH_3$ stretching

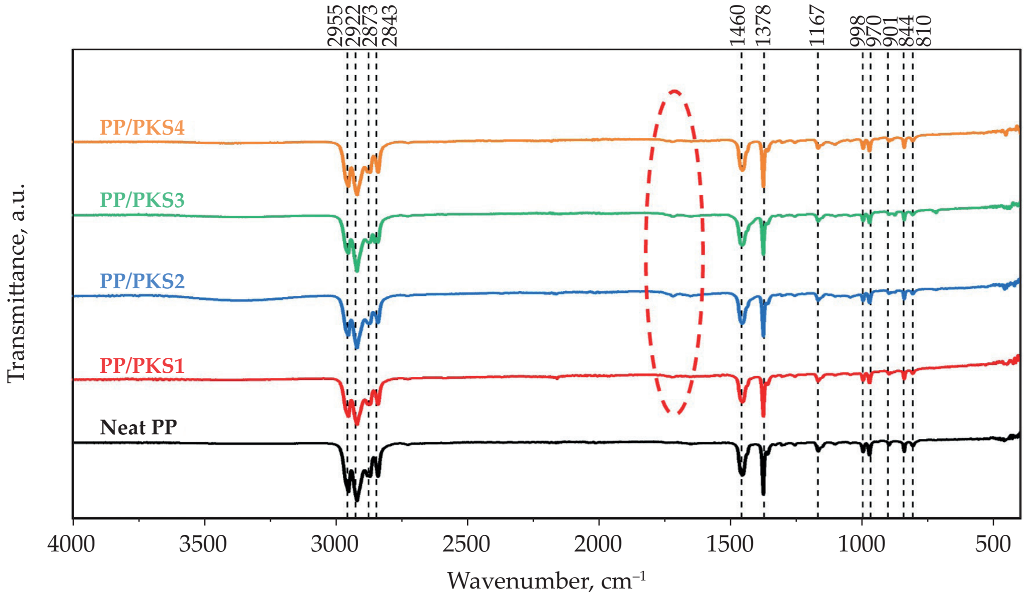

Fig. 2. ATR-FT-IR spectra of the pure PP and PP micro-composites

peaks at 2955 and 2873 cm^{-1}, $-CH_2$ stretching peaks at 2922 and 2843 cm^{-1}, as well as the methyl group umbrella mode at 1378 cm^{-1}. The other groups from the FT-IR spectrum results, as shown in Table 2, show parts of the functional groups in polypropylene.

In this study, the AC was standardized to a uniform size by passing through a 200-mesh sieve (74 μm). This procedure aims to provide uniformity of particle dispersion in the matrix. Figure 3 presents surface images of PP micro-composites at a magnification of 5000×. The surface morphology and distribution of AC fillers in PP micro-composites are depicted clearly in this figure. The image of all samples exhibits a smooth surface. Except for PP/PKS4, the AC filler is uniformly distributed within the PP polymer, indicating the absence of agglomeration and no evidence of air entrapment in the sample.

In the PP/PKS4, AC tends to agglomerate. The formation of agglomerations may result from carbon clumping, attributed to the incorporation of extra AC filler. The agglomeration area may lead to variations in the characteristic properties of the sample, including electrical conductivity and mechanical test results, compared to other regions. Visually, increased amounts of AC fillers result in a darker coloration of the sample.

T a b l e 2. Wavenumbers of functional groups [16]

Wavenumber, cm^{-1}	Functional groups
2955; 2873	$-CH_3$ stretching
2922; 2843	$-CH_2-$ stretching
1460	$-CH_2-$ scissor
1378	$-CH_3$ symmetric deformation
1167	C-H wagging
998	$-CH_3$ asymmetric rocking
974; 940	C-C stretching
844; 810	$-CH_2-$ rocking

The electrical resistivity (ϱ) of pure PP and PP micro-composites is presented in Table 3. A significant reduction in resistivity was seen following the incorporation of AC particles into the PP matrix. This phenomenon may be attributed to the potential formation of an AC network in the PP micro-composites. The establishment of this network within the PP micro-composites induces an electrical percolation threshold. When AC particles are in close alignment and interconnected, a three-dimensional conductive pathway is established due to the electrical conductivity of the AC. Consequently, as the AC content

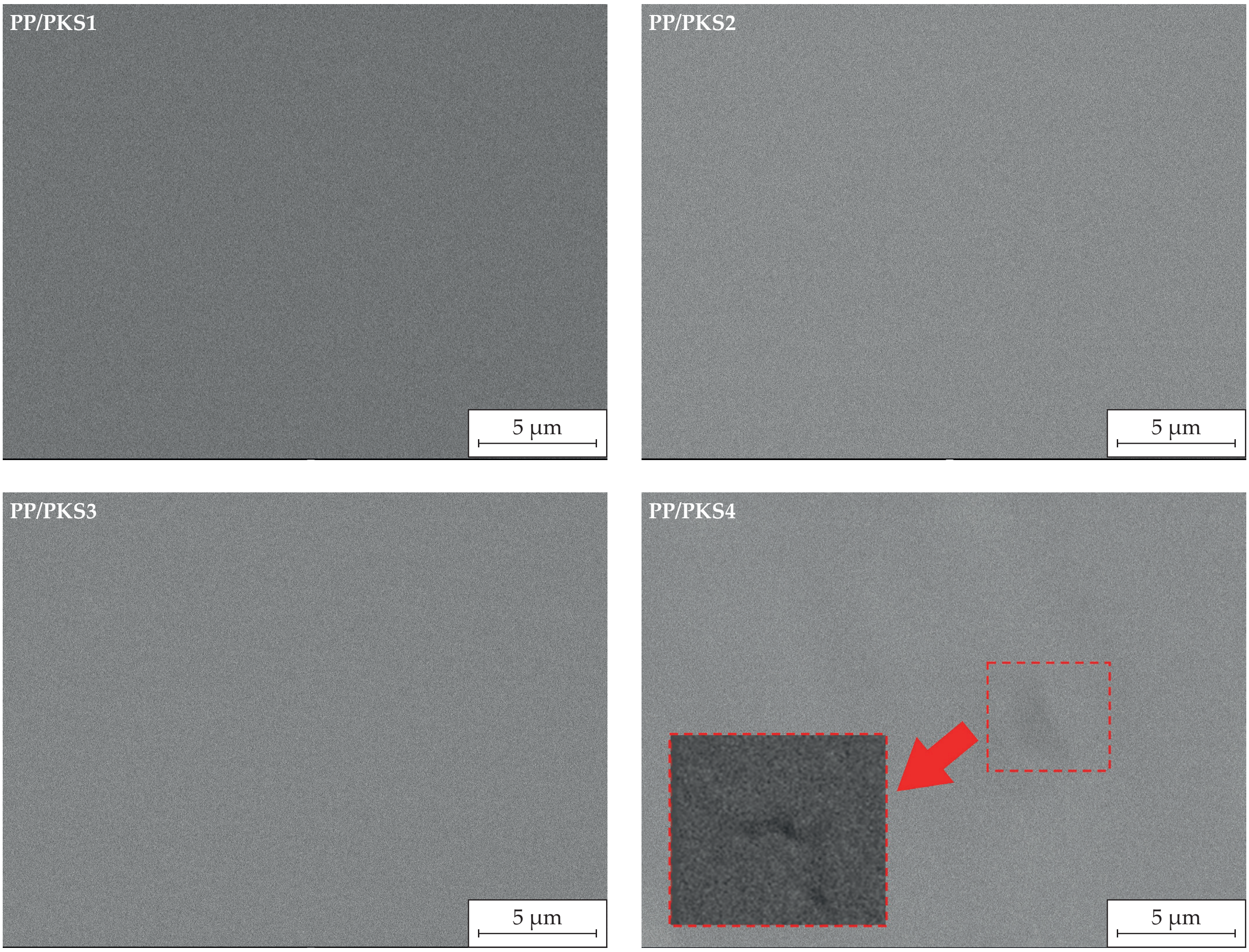

Fig. 3. SEM images of PP micro-composites

T a b l e 3. Electrical resistivity and conductivity of PP micro-composites

Sample	Average resistance, Ω	Resistivity, Ω · m	Conductivity, S/m
Pure PP	1.76×10^{18}	9.62×10^{14}	1.04×10^{-15}
PP/PKS1	1.49×10^{16}	8.14×10^{12}	1.23×10^{-13}
PP/PKS2	6.70×10^{14}	3.66×10^{11}	2.73×10^{-12}
PP/PKS3	4.29×10^{13}	2.34×10^{10}	4.26×10^{-11}
PP/PKS4	2.29×10^{12}	1.25×10^{9}	8.01×10^{-10}

rises, the electron flows through the PP micro-composite samples similarly escalate, leading to a reduction in the resistivity of the PP micro-composites. Comparable results have been documented previously [17, 18]. Table 3 also indicates a rise in electrical conductivity due to the presence of AC. Incorporating 4wt% AC elevated the electrical conductivity to 8.01×10^{-10} S/m, in contrast to the pure PP, which measured 1.04×10^{-15} S/m.

Pang *et al*. [19] explained that polymers exhibiting resistivity values between 10^4–10^9 Ω · m or electrical conductivity values between 10^{-9}–10^{-4} S/m possess an electrostatic dissipative level. This level can transmit electrical charges, allowing electron mobility inside the plastic and preventing the accumulation of static electric charge when the plastic is in contact with other substances. Polymers may be formulated as antistatic packing materials within this electrical resistivity range.

As shown in Figure 4, incorporating AC within the PP matrix at a composition range of 0–4 wt% has not demonstrated the limitations of the composite's efficacy as an antistatic material. The electrical conductivity with a composition of 4 wt% exhibits the highest value in this range, which is 8.01×10^{-10} S/m, a value that approaches the minimum limit described by Pang *et al*., which is 10^{-9} S/m [19]. However, Figure 4 indicates that the enhancement in conductivity persists with the addition of AC fraction. Incorporating AC from PKS into PP may facilitate the development of an antistatic packaging material.

Table 4 indicates that incorporating AC fillers tends to enhance tensile strength at the expense of elongation. The increase in tensile strength of PP may be attributed to the characteristics of the filler, which facilitate strong bonding between PP and carbon. PP/PKS3 exhibits a maximum tensile strength of 36 MPa. The increased AC subsequently demonstrates a reduction in tensile strength, as evidenced by PP/PKS4 sample (35 MPa). This phenomenon may be attributed to AC starting to undergo agglomeration, as depicted in Figure 3.

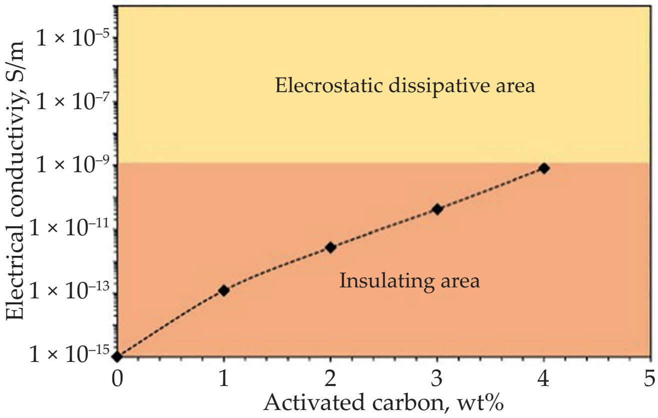

Fig. 4. PP micro-composites in the classification of materials according to their electrical conductivity

The presence of AC significantly reduces the elongation of PP. This significant reduction in elongation may be attributed to the reduced chain mobility of PP, as the presence of AC constrained the free volume [20, 21]. The decrease in elongation among the PP/PKS1, PP/PKS2, and PP/PKS3 samples appears relatively similar at first glance. Additionally, the elongation of PP/PKS4 exhibited a notable decrease, with the elongation at break recorded at 70.33%. Once more, this phenomenon may be connected to the fact that AC began to undergo agglomeration in PP/PKS4. It can be highlighted that the addition of AC increases the brittleness of polypropylene.

DSC thermograms of pure PP and PP micro-composites are shown in Figure 5. No significant effect of AC on the melting point of PP was found (Table 5). Chafidz *et al.* (2016) also reported a similar phenomenon [22]. Moreover, the incorporation of AC into the PP matrix increased the melting enthalpy due to higher crystallinity. It can be explained that AC acts as a foreign particle and its presence facilitates the growth of nucleation in the matrix and intermolecular interactions, thus increasing the crystallinity of PP [22]. However, there is a slight decrease in the degree of crystallinity in PP/PKS4. This may be related to the occurring agglomeration, which means that its role as a nucleating agent is not optimal (Fig. 3).

Thermogravimetric analysis (TGA) and derivative thermogravimetry (DTG) were conducted to investigate the impact of AC incorporation on the thermal stability of the micro-composites. Figure 6 illustrates the results

T a b l e 4. Mechanical properties of pure PP and PP micro-composites

Sample	Tensile strength MPa	Elongation at break, %
Pure PP	30.68±1.20	105.92±3.25
PP/PKS1	32.14±0.75	80.35±2.31
PP/PKS2	35.39±0.82	78.83±1.15
PP/PKS3	36.42±0.55	76.67±1.25
PP/PKS4	35.23±0.22	70.33±0.65

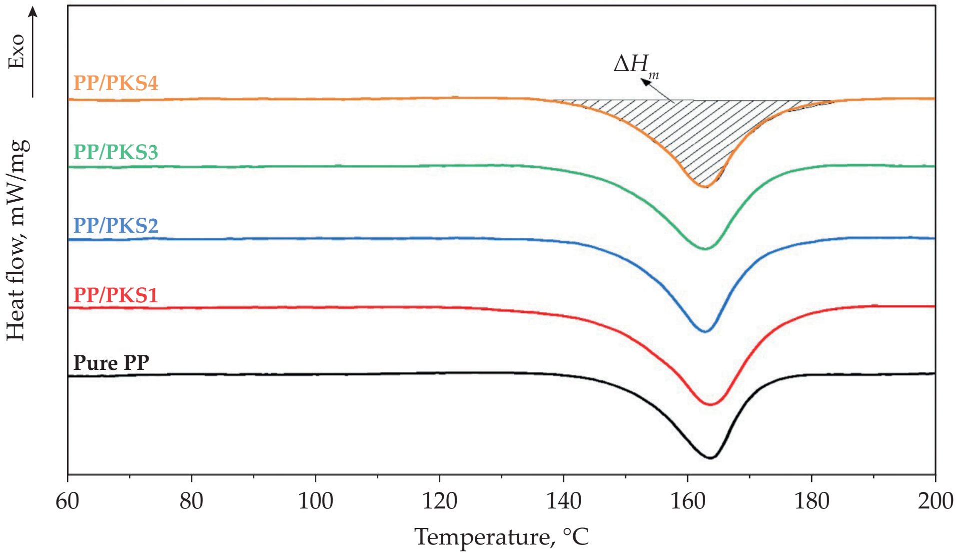

Fig. 5. DSC thermograms of PP and PP micro-composites

Table 5. Thermal properties of pure PP and PP micro-composites

Sample	T_m, °C	ΔH_m, J/g	X_c, %
Pure PP	164.3	51.8	25.02
PP/PKS1	163.3	53.6	26.16
PP/PKS2	163.8	54.1	26.67
PP/PKS3	163.4	54.5	27.14
PP/PKS4	163.4	53.5	26.92

of the TGA and DTG analysis. The thermal degradation of pure PP and PP micro-composites transpires through a single-step process. As seen in Figure 6, the presence of AC appeared to slow down the thermal degradation of PP. The onset temperature degradation of PP enhanced in the presence of AC, as compared to pure PP. This characteristic is associated with the thermal stability of PP which increases with the presence of AC.

It may be explained that the improvement in thermal stability of the micro-composites is due to a network structure established by the interfacial interaction between PP chains and AC fillers, leading to an elevation in the activation energy required for the onset of the degradation process. An additional explanation is that the AC acts as an insulator or barrier that impedes the diffusion of volatile compounds from the polymer matrix into the gas phase during degradation [22, 23].

CONCLUSIONS

Activated carbon was successfully synthesized from palm kernel shell waste and used as a filler for PP micro-composites through mixing in m-xylene. AC can be evenly dispersed in the PP matrix using this method. Tensile strength of micro-composites increases with the addition of AC, resulting in a reduction of elongation, due to increased brittleness. The melting temperature of PP was not affected by the addition of AC. However, there is a tendency for an increase in enthalpy and the crystallinity degree. The presence of AC simultaneously increases PP's thermal stability and electrical conductivity. However, PP micro-composites do not reach the required threshold to dissipate electrostatic charges and therefore cannot be used as antistatic packaging materials.

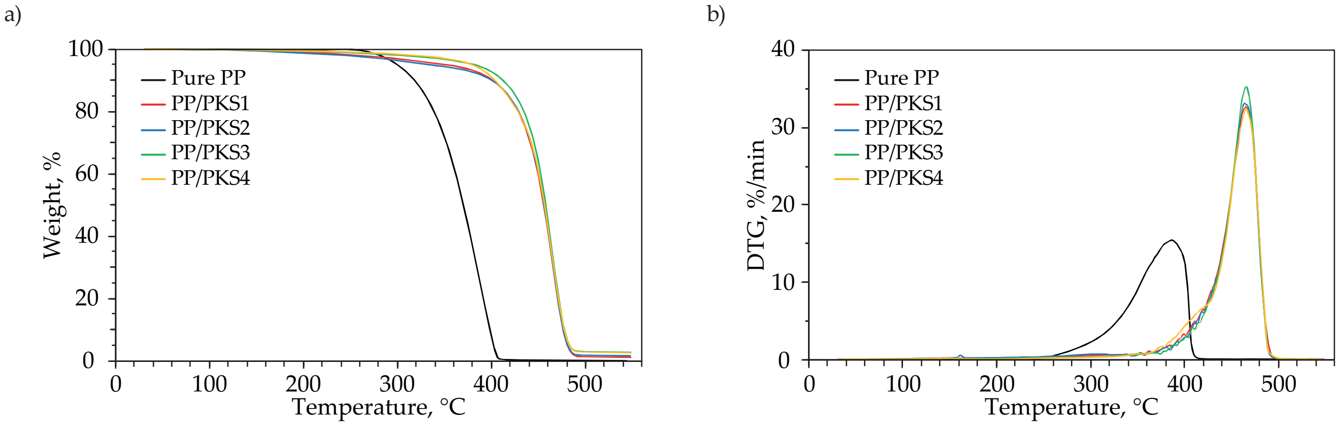

Fig. 6. Thermogravimetric curves of PP and micro-composites: a) TGA, b) DTG

Authors contribution

M.K. – conceptualization, methodology, supervision, data analysis, writing review and editing; S.D. – methodology, writing review and editing; M.R.H.W – experimental work, collecting data, data analysis, project administration; N.Y.F – experimental work, collecting data, data analysis, project administration; J.W. – methodology, writing review and editing. All authors have agreed to the published version of the paper.

Funding

This research was funded by Universitas Sebelas Maret through a scheme of Hibah Grup Riset grant 2024 with contract number 194.2/UN27.22/PT.01.03/2024.

Conflict of interest

There is no conflict of interest in the publication of this paper.

REFERENCES

[1] Cho M.K., Song I., Pavlidis S. *et al*.: *IEEE Transactions on Nuclear Science* **2018**, *65(1)*, 426. https://doi.org/10.1109/TNS.2017.2778946

[2] Dilkes-Hoffman L.S. Lane J.L., Grant T. *et al*.: *Journal of Cleaner Production* **2018**, *180*, 325. https://doi.org/10.1016/j.jclepro.2018.01.169

[3] Foltynowicz Z.: *Polimery* **2020**, *65(1)*, 3. https://doi.org/10.14314/polimery.2020.1.1

[4] Hossain M.T. Shahid A., Mahmud N. *et al*.: *Discover Nano* **2024**, *19(1)*, 2, https://doi.org/10.1186/s11671-023-03952-z

[5] Obasi H.C., Mark U.C., Mark U.: *Composites and Advanced Materials* **2021**, *30*. https://doi.org/10.1177/26349833211007497

[6] Krajewski D. Oleksy M., Oliwa R. *et al*.: *Polimery* **2024**, *69(7-8)*, 413. https://doi.org/10.14314/polimery.2024.7.3

[7] Shohih E.N., Kaavessina M., Distantina S.: *AIP Conference Proceedings,* **2020**, *2296*, 020062. https://doi.org/10.1063/5.0030590

[8] Mamunya Y., Misiura A., Godzierz M. *et al*.: *Polymers* **2024**, *16(6)*, 741. https://doi.org/10.3390/polym16060741

[9] da Silva T.F., Menezes F., Montagna L.S. *et al*.: *Journal of Applied Polymer Science* **2019**, *136(13)*, 47273. https://doi.org/10.1002/app.47273

[10] Huang Y., Kormakov S., He X. *et al*.: *Polymers* **2019**, *11(2)*, 187. https://doi.org/10.3390/polym11020187

[11] Tarhini A., Tehrani-Bagha A.R.: *Applied Composite Materials* **2023**, *30(6)*, 1737. https://doi.org/10.1007/s10443-023-10145-5

[12] Agustiar, Romano, Aulia M.R. *et al*.: *IOP Conference Series: Earth and Environmental Science*, **2024**, *1297*, 012076. https://doi.org/10.1088/1755-1315/1297/1/012076

[13] Aktawan A., Maryudi, Siti S. *et al*.: *Key Engineering Materials* **2020**, *849*, 3. https://doi.org/10.4028/www.scientific.net/KEM.849.3

[14] Uchegbulam I., Momoh E.O., Agan S.A.: *Cleaner Materials* **2022**, *6*, 100154, https://doi.org/10.1016/j.clema.2022.100154

[15] Przepiórski J., Skrodzewicz M., Morawski A.W.: *Applied Surface Science* **2004**, *225(1-4)*, 235. https://doi.org/10.1016/j.apsusc.2003.10.006

[16] Socrates G.: "Infrared and Raman Characteristic Group Frequencies: Tables and Charts", 3rd ed., John Wiley and Sons. Ltd., Chichester 2004, p. 50-100.

[17] Dungani R., Aditiawati P. Alamsyah E.M. *et al*.: *Case Studies in Chemical and Environmental Engineering* **2024**, *10*, 100948. https://doi.org/10.1016/j.cscee.2024.100948

[18] Angin N., Ertas M., Caylak S. *et al*.: *Sustainable Materials and Technologies* **2023**, *37*, e00655. https://doi.org/10.1016/j.susmat.2023.e00655

[19] Pang H., Xu L., Yan D.X. *et al*.: *Progress in Polymer Science* **2014**, *39(11)*, 1908. https://doi.org/10.1016/j.progpolymsci.2014.07.007

[20] Kaavessina M., Chafidz A., Ali A. *et al*.: *Journal of Elastomers and Plastics* **2015**, *47(8)*, 753. https://doi.org/10.1177/0095244314557973

[21] Rifa'i A.F., Kaavessina M., Distantina S.: *Periodica Polytechnica Chemical Engineering* **2025**, *69(1)*, 149. https://doi.org/10.3311/PPch.37876

[22] Chafidz A., Hamdan Latief F., Al-Fatesh A.S. *et al*.: *Philosophical Magazine Letters* **2016**, *96(10)*, 367. https://doi.org/10.1080/09500839.2016.1213441

[23] Kaavessina M., Rifa'i A.F., Distantina S. *et al*.: *Journal of Polymer Research* **2025**, *32(2)*, 59. https://doi.org/10.1007/s10965-025-04280-9

Received 28 XI 2024.
Accepted 25 II 2025.